

## Interdiffusion in Critical Binary Mixtures by Molecular Dynamics Simulation

Kurt Binder,<sup>1</sup> Subir K. Das,<sup>2</sup> Michael E. Fisher,<sup>2</sup> Jürgen Horbach,<sup>3</sup> Jan V. Sengers<sup>2</sup>

<sup>1</sup> Institut für Physik, Johannes Gutenberg Universität, Germany

<sup>2</sup> Institute for Physical Science and Technology, University of Maryland, USA

<sup>3</sup> Institut für Materialphysik im Weltraum, Deutsches Zentrum für Luft- und Raumfahrt, Germany

Corresponding author:

Kurt Binder

Institut für Physik

Johannes Gutenberg Universität Mainz

Staudinger Weg 7

55099 Mainz, Germany

E-Mail: kurt.binder@uni-mainz.de

### Abstract

A simulation study of the static and dynamic critical behavior of a symmetric binary Lennard-Jones mixture is briefly reviewed. Using a combination of semi-grand-canonical Monte Carlo (SGMC) and molecular dynamics (MD) methods near the critical temperature of liquid-liquid unmixing, the correlation length and “susceptibility” related to the critical concentration fluctuations are estimated, as well as the self- and interdiffusion coefficients. While the self-diffusion coefficient does not show a detectable critical anomaly, the interdiffusion coefficient is found to vanish when one approaches the critical temperature at fixed critical concentration. It is shown that in the corresponding Onsager coefficient both a divergent singular part and a nonsingular background term need to be taken into account. With appropriate finite-size scaling analysis (the particle numbers studied for the dynamics lie only in the range from  $N = 400$  to  $6400$ ), the critical behavior of the interdiffusion coefficient is found to be compatible both with the theoretically predicted behavior and with corresponding experimental evidence.

Keywords: fluid binary mixtures; critical behavior; Monte Carlo method; molecular dynamics simulation; self-diffusion coefficient; interdiffusion coefficient; Onsager coefficient

### 1. Introduction

The interplay of static structure and transport coefficients in fluid and solid binary mixtures has been a topic of longstanding interest [1-6]. Understanding this problem is crucial for ionic conductors [1], disordered metallic alloys [2,5] and the phase separation processes [5] that these systems may undergo, dynamics of glassforming fluids [6], ordering phenomena occurring in monolayers adsorbed on surfaces affected by surface

© 2007, K. Binder

Diffusion Fundamentals 6 (2007) 10.1 - 10.12

diffusion [3,7], etc. A particularly popular concept (e.g., [2]) is the idea to find simple relations between self-diffusion coefficients, which characterize the diffusive motion of “tagged” particles in a mixture, and the interdiffusion coefficient, which describes how concentration gradients spread out. However, even for simple lattice-gas type models this idea is still subject to controversy (e.g. [8,9]).

Fluid binary mixtures near the critical point of a miscibility gap in their phase diagram are clearly an example where a simple relation between self-diffusion and interdiffusion coefficients does not exist. According to the conventional van Hove theory of critical slowing down [10,11] the interdiffusion constant  $D_{AB}$  of a binary ( $A,B$ ) mixture would have the same singularity as the inverse of the susceptibility  $\chi$  describing the concentration fluctuations in the mixture. In terms of the well-known partial structure factors  $S_{\alpha\beta}(q)$  [6] of binary systems ( $\alpha,\beta = A,B$ ;  $q$  is the wave number),  $\chi$  is defined by

$$S^{cc}(q) = k_B T \chi / [1 + q^2 \xi^2 + \dots], \quad (1)$$

$$S^{cc}(q) \equiv (1 - x_A)^2 S_{AA}(q) + x_A^2 S_{BB}(q) - 2x_A(1 - x_A) S_{AB}(q). \quad (2)$$

Here  $k_B$  is Boltzmann’s constant,  $T$  the absolute temperature, and  $\xi$  is the correlation length of the concentration fluctuations, while  $x_A$  ( $x_B = 1 - x_A$ ) are the relative concentrations of  $A$  ( $B$ ) particles in the mixture. The interdiffusion coefficient then can be written as

$$D_{AB} = \Lambda(T) / \chi, \quad (3)$$

where according to the van Hove conventional theory the Onsager coefficient  $\Lambda(T)$  is finite at the critical temperature  $T_c$  of the mixture. The interdiffusion coefficient vanishes since  $\chi$  diverges according to a power law (as well as  $\xi$ ), for  $x_A = x_B = 1/2$  being the critical concentration of a symmetric binary mixture,

$$\chi = \Gamma \varepsilon^{-\gamma}, \quad \xi = \xi_0 \varepsilon^{-\nu}, \quad \varepsilon = (T - T_c) / T_c. \quad (4)$$

Here  $\Gamma$ ,  $\xi_0$  are critical amplitudes, and  $\gamma, \nu$  the associated critical exponents [12]. Binary mixtures belong to the Ising universality class [12], for which, in  $d = 3$  dimensions [13,14]

$$\gamma \approx 1.239, \quad \nu \approx 0.629. \quad (5)$$

While the van Hove conventional theory is believed to hold for solid binary mixtures [10,11,15], both mode coupling theory [16-20] and renormalization group theory [10,21,22] imply that it fails for fluid binary mixtures near their critical point. In particular, it was found that  $\Lambda(T)$  contains a singular part  $\Delta\Lambda(T)$  in addition to a non-critical background term  $\Lambda_b(T)$ ,

$$\Lambda(T) = \Lambda_b(T) + \Delta\Lambda(T), \quad \Delta\Lambda(T) = L_0 \varepsilon^{-\nu_\lambda}, \quad (6)$$

$L_0$  being a critical amplitude, and the exponent  $\nu_\lambda$  is related to the exponent  $\eta = 2 - \gamma/\nu$  describing the decay of critical correlations [12] and the exponent  $x_\eta$  describing the

critical divergence of the shear viscosity  $\eta^*$ , which exhibits a so-called multiplicative anomaly [10,11,19]

$$\nu_\lambda = x_\lambda \nu, \text{ with } x_\lambda = 1 - \eta - x_\eta, \quad (7)$$

$$\eta^* = \eta_0 \varepsilon^{-x_\eta}, \quad x_\eta \approx 0.068, \quad (8)$$

$\eta_0$  being a critical amplitude prefactor. Since  $\eta \approx 0.03$  one predicts  $\nu_\lambda = 0.567$ . In fact, precise experimental data consistent with these results have existed for a long time [23]!

However, no experiments exist where both self-diffusion and interdiffusion coefficients are available near the critical point of a fluid binary mixture. In fact, no pronounced critical anomaly is expected theoretically for the self-diffusion constants  $D_A, D_B$ , and this expectation is consistent with simulation studies of lattice-gas models [24]. Nevertheless it is interesting to reconsider the problem of interdiffusion and self-diffusion in critical binary mixtures via computer simulation again in view, in particular, of recent results [25] claiming that the vanishing of  $D_{AB}$  is inconsistent with Eqs. (6-8).

In the present paper, we hence review a recent study [26,27] where a symmetric binary Lennard-Jones mixture near its critical point has been extensively studied: combining semi-grand-canonical Monte Carlo (SGMC) methods [28-30] with microcanonical molecular dynamics (MD) runs [31] one can study transport phenomena in model systems in which long-wavelength concentration fluctuations are well equilibrated [32]. In this way, reliable information both on static critical properties {Eqs. (1), (4)} and the transport properties (interdiffusion coefficient {Eq.(3)}, shear viscosity {Eq.(8)}, and the self-diffusion coefficients) can be obtained for the model system studied. Of course, simulations always deal with systems of finite size (particle numbers  $400 \leq N \leq 12800$  were studied [26,27]) and hence a careful assessment of finite-size effects near the critical point is necessary, applying finite-size scaling concepts [33-35].

## 2. Model and Simulation Techniques

We consider a binary fluid of point particles with pair-wise interactions in a box of volume  $V = L^3$  with periodic boundary conditions. The Lennard-Jones potential

$$\phi_{LJ}(r_{ij}) = 4\varepsilon_{\alpha\beta} [(\sigma_{\alpha\beta}/r_{ij})^{12} - (\sigma_{\alpha\beta}/r_{ij})^6] \quad (9)$$

is truncated at  $r_{ij} = r_c$  and modified there to create a potential that is everywhere continuous and also has a continuous first derivative,

$$u(r_{ij}) = \phi_{LJ}(r_{ij}) - \phi_{LJ}(r_c) - (r_{ij} - r_c) \left. \frac{d\phi_{LJ}}{dr_{ij}} \right|_{r_{ij}=r_c} \quad (10)$$

for  $r_{ij} < r_c$  while  $u(r_{ij} \geq r_c) \equiv 0$ . The range parameters in Eq. (9) were chosen as  $\sigma_{AA} = \sigma_{BB} = \sigma_{AB} = \sigma$ , while the cutoff was set at  $r_c = 2.5 \sigma$ . The particle number  $N = N_A + N_B$  and the volume are chosen to yield a reduced density  $\rho^* = \rho\sigma^3 = N\sigma^3/V = 1$ . Then neither crystallization nor the liquid-vapor transition is a problem, at the temperatures of interest. Finally, the reduced temperature  $T^* = k_B T/\varepsilon_0$  and energy parameters are chosen as [26,27,32]  $\varepsilon_{AA} = \varepsilon_{BB} = 2 \varepsilon_{AB} = \varepsilon_0$ . For equilibration, first a MC run is carried out in the

canonical ensemble ( $N_A = N_B$ ,  $V$ ,  $T$ ) starting from particles at random positions. The MC moves tried are random displacements of randomly chosen single particles, applying the standard Metropolis method [31,36]. After about  $10^4$  Monte Carlo steps (MCS) per particle, the equilibration is continued by the SGMC method [26-30,32]: after 10 displacement steps per particle  $N/10$  particles are randomly chosen successively, and an identity switch in general is controlled both by the energy change,  $\Delta E$ , and the chemical potential difference,  $\Delta\mu$ , between the particles. However, since we wish to simulate states with an average concentration  $\langle x_A \rangle = \langle x_B \rangle = 1/2$  (with  $x_\alpha = N_\alpha/N$ ) for  $T > T_c$ , we chose  $\Delta\mu = 0$ . For  $T < T_c$ , this choice yields states either along the A-rich or the B-rich branch of the coexistence curve in the  $(T, x_A)$ -plane.

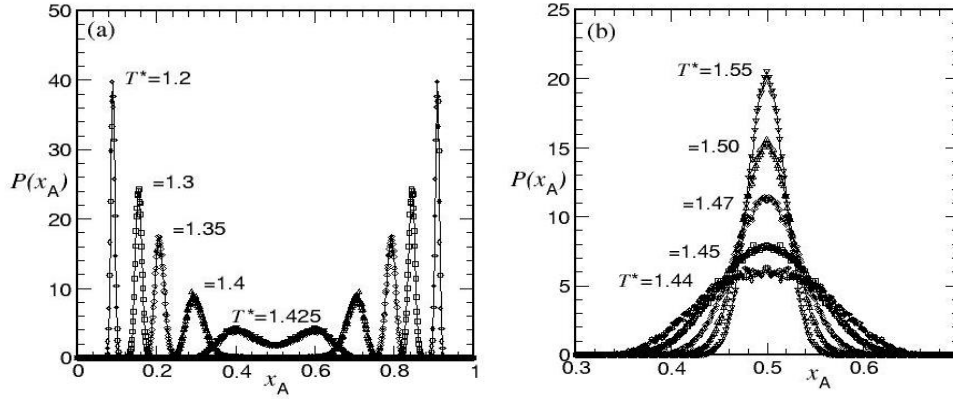


Fig.1: Probability distribution  $P(x_A)$  of the relative concentration  $x_A = N_A/N$  of  $A$ -particles for  $N = 6400$ ,  $\Delta\mu = 0$ , at several temperatures (a) below  $T_c$  and (b) above  $T_c$ . From S. K. Das et al. [27].

In the SGMC method the concentration  $x_A$  is a fluctuating variable, and hence the probability distribution  $P(x_A)$  is straightforwardly sampled. Since  $P(x_A) = P(1-x_A)$  for  $\Delta\mu = 0$ , the coexistence curve (for  $T < T_c$ ) is obtained as

$$x_A^{coex(1)} = (1 - \langle x_A \rangle), \quad x_A^{coex(2)} = \langle x_A \rangle, \quad (11)$$

where moments  $\langle x_A^k \rangle$  are defined by

$$\langle x_A^k \rangle = 2 \int_{1/2}^1 x_A^k P(x_A) dx_A. \quad (12)$$

The concentration susceptibility  $\chi$  is then obtained from the second moment via

$$k_B T \chi = N (\langle x_A^2 \rangle - 1/4), \quad T > T_c. \quad (13)$$

For the accurate location of the critical temperature, it is useful to record the fourth-order cumulant  $U_L$  [34]

$$U_L = \langle (x_A - 1/2)^4 \rangle / [\langle (x_A - 1/2)^2 \rangle^2]. \quad (14)$$

Fig. 1 shows “raw data” of the simulation for  $P(x_A)$  for various temperatures  $T^*$ , while Fig. 2 illustrates the estimation of the critical temperatures from intersections of cumulants for different sizes  $N$  [27]. Note that in the finite-size scaling limit ( $L \rightarrow \infty$ ,  $\xi \rightarrow \infty$ ,  $L/\xi$  finite) these cumulants should intersect at  $T_c$  in a value, which (for a given universality class and type of system shape and boundary conditions) is universal [34]. The data indeed are consistent with a unique intersection point at  $T_c^* = 1.4230 \pm 0.0005$  with the predicted value [37]  $U_L(T_c^*) \approx 0.6236$  for the Ising universality class.

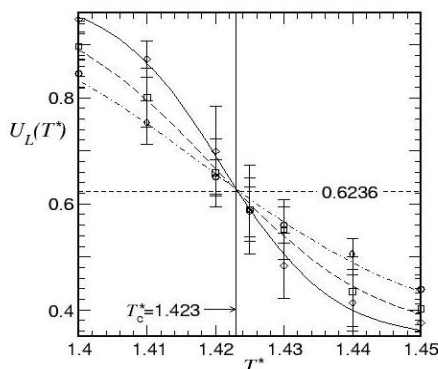


Fig. 2: The fourth-order cumulant  $U_L(T)$  plotted vs.  $T^*$  for  $N = 1600$  (circles), 3200 (squares) and 6400 (diamonds). The vertical straight line indicates the resulting estimate for  $T_c^*$ , while the horizontal broken straight line indicates the theoretical value that  $U_L(T = T_c^*)$  should take, for the Ising universality class. From Das et al. [27].

The advantage of the SGMC method is not only the relative ease with which  $P(x_A)$  and its moments are obtained, allowing then a reliable estimation of  $T_c$ , the coexistence curve {Eq. (11)} and  $\chi$  {Eq. (13)}; a crucial further advantage is that long wavelength concentration fluctuations are rather well equilibrated, since critical slowing down near  $T_c$  is somewhat less of a problem than it would be for other simulation methods. The critical divergence of the largest relaxation time  $\tau_{max}$  is, of course, always rounded off in a simulation due to finite system size and one expects

$$\tau_{max} \propto L^z, \quad T = T_c, \quad (15)$$

where the dynamic exponent  $z$  depends on the “dynamic universality class” [10].

For a MC simulation in the canonical ensemble the critical unmixing transition falls into “class D” of the Hohenberg-Halperin classification [10], for which  $z = 4 - \eta$ , while for the SGMC we have “class C” [10] for which  $z \approx 2$ . Clearly the numerical effort for equilibrating the system in the canonical ensemble would be prohibitively large, since the time over which averages are taken should exceed  $\tau_{max}$  by several orders of magnitude.

Also using MD exclusively (both for equilibration and for a study of the critical dynamics) is problematic, since the predicted dynamic exponent is [10]  $z \approx 3$ . Note that MD realizes the microcanonical NVE ensemble (internal energy  $E$  being strictly conserved) and then it is difficult to fine-tune the temperature (which would be a fluctuating observable of the simulation [31]). Using the standard recipe of isothermal MD simulations via the coupling of the system to suitable “thermostats” [31] slightly disturbs the (otherwise Newtonian) equations of motions and hence leads to some systematic errors, when dynamic correlations are recorded. Such errors are likely to be significant near criticality.

All these problems are avoided by the present technique where an ensemble of initial states at the desired temperature is created by SGMC methods, and starting MD runs in the NVE ensemble from these initial states enables well-defined canonical averages of time-displaced correlation functions to be computed [26,27,32]. We choose the masses of the particles identical ( $m_A = m_B = m$ ), apply the velocity Verlet algorithm [31] with a time step  $\delta t^* = 0.01 / \sqrt{48}$  where  $t^* = t/t_0$  with the MD time scale  $t_0$  being set by  $t_0 = (m \sigma^2 / \varepsilon_0)^{1/2}$ . We used about  $10^6$  MD steps for  $T^* = 1.5$  and higher, and up to  $2.8 \times 10^6$  MD steps for  $T$  closer to  $T_c$ . Within this time scale, no systematic temperature drift occurs, and we think that discretization errors are still well under control.

Self-diffusion constants  $D_A, D_B$  are then extracted simply from the mean-square displacements of tagged particles

$$g_A(t) = \left\langle [\vec{r}_{iA}(0) - \vec{r}_{iA}(t)]^2 \right\rangle \quad (16)$$

by applying the Einstein relation

$$D_A^* = (t_0 / \sigma^2) \lim_{t \rightarrow \infty} [g_A(t) / 6t], \quad (17)$$

and similarly for  $D_B^*$ . Note that for the computation of Eq. (16), a second set of coordinates (with no periodic boundary conditions) is used, so the displacements are not restricted by the size of the simulation box, and can grow without limit. For  $T > T_c$  and  $\Delta\mu = 0$  we have  $\langle x_A \rangle = \langle x_B \rangle = 1/2$ , of course, and then the symmetry of the model requires  $g_A(t) = g_B(t)$  and  $D_A^* = D_B^*$ . To gain statistics, the average in Eq. (16) thus includes an average over all the particles.

The interdiffusion constant is estimated from Eq. (3) and the Green-Kubo relation [38]

$$\Lambda(T) = (t_0 / N\sigma^2 T^*) \int_0^\infty dt \langle J_x^{AB}(0) J_x^{AB}(t) \rangle, \quad (18)$$

in which the current vector  $\vec{J}^{AB}$  is defined by

$$\vec{J}^{AB}(t) = (1 - x_A) \sum_{i=1}^{N_A} \vec{v}_{i,A}(t) - x_B \sum_{i=1}^{N_B} \vec{v}_{i,B}(t), \quad (19)$$

where  $\vec{v}_{i,\alpha}(t)$  denotes the velocity of particle  $i$  of type  $\alpha$  at time  $t$ . The shear viscosity is also obtained from a corresponding relation [26,27,32,38].

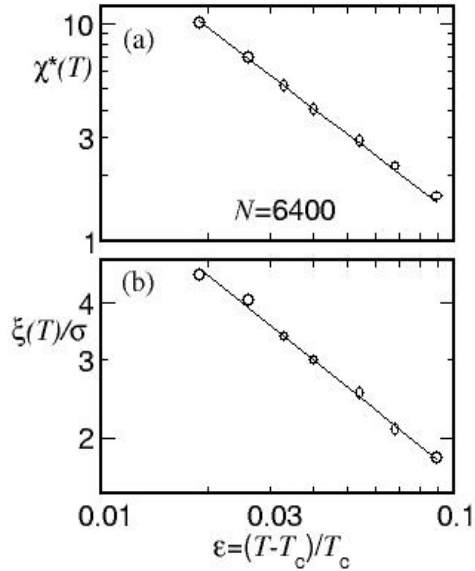


Fig 3: Log-log plot of (a) the reduced susceptibility  $\chi^* = \epsilon_0 \chi$  and (b) the reduced correlation length  $\xi(T)/\sigma$  vs.  $\epsilon$ . The lines represent fits using the anticipated Ising exponents. All data refer to systems of  $N = 6400$  particles. From Das et al. [27].

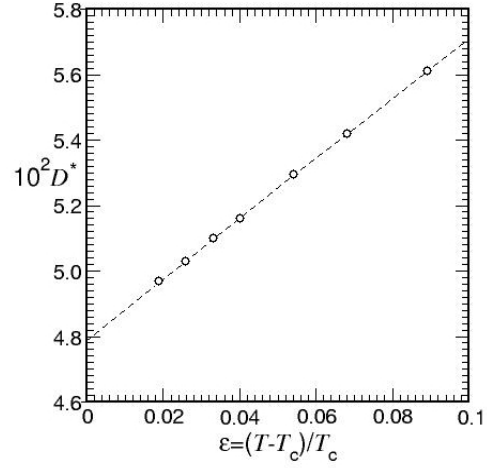


Fig. 4: Variation of the reduced self-diffusion coefficient with temperature, using data for  $N = 6400$  at  $x_A = x_B = 1/2$ . From Das et al. [27].

### 3. Results for Static and Dynamic Critical Properties

From the distribution  $P(x_A)$  the ‘‘concentration susceptibility’’  $\chi$  has been extracted [26,27], paying careful attention to finite-size effects via a finite-size scaling analysis. From the partial structure factors, using Eqs. (1), (2), and the known  $\chi$ , estimates for  $\xi$  have also been extracted. Fig. 3 shows the final results of this analysis. It is seen that both  $\chi$  and  $\xi$  (and also the order parameter  $x_A^{coex(2)} - x_A^{coex(1)}$  [27]) are very well compatible

with the expected Ising critical behavior, although due to finite-size effects only data for  $\varepsilon \geq 0.02$  are available.

Fig. 4 shows results for the self-diffusion coefficient: it decreases weakly and linear with temperature as the critical point is approached. No detectable sign of a critical anomaly can be seen. Similarly, a study of self-diffusion near the vapor-liquid critical point of a lattice-gas model did not find a critical anomaly either [24] (although this model belongs to “class B” in the Hohenberg-Halperin classification [10]).

The Onsager coefficient  $\Lambda(T)$  for interdiffusion is shown in Fig. 5. While far above  $T_c$  the Onsager coefficient has only a very weak temperature dependence, there occurs a sharp rise when  $T_c$  is approached. These data clearly demonstrate that the simple van Hove description (implying a finite nonsingular  $\Lambda(T_c)$ ) is invalid:  $\Lambda(T)$  must contain both a critical part and a non-critical background term [which dominates far above  $T_c$ ], as specified in Eq. (6).

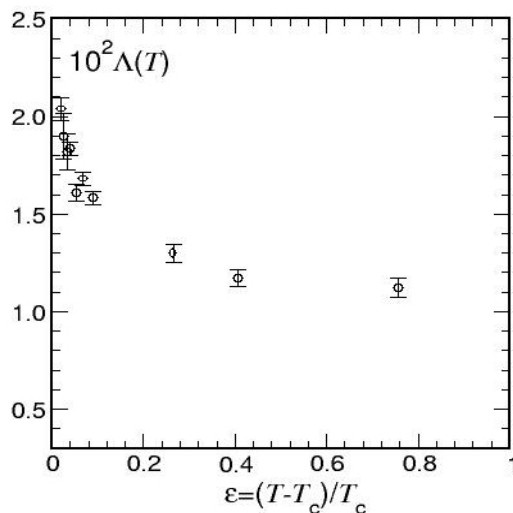


Fig. 5: Onsager coefficient  $\Lambda(T)$  for interdiffusion plotted vs. temperature, for a system of  $N = 6400$  particles. From Das et al. [27].

However, most of our simulation results are in a temperature regime where the effect of the non-singular background is by no means negligible. As a result, when one analyzes directly the critical behavior of  $D_{AB}$  in a naïve way, e.g. by a log-log plot of  $D_{AB}$  versus  $\varepsilon$ , one expects to see a crossover from an exponent  $\gamma = 1.239$  for  $\varepsilon \geq 0.4$  [where  $\Lambda(T)$  in Fig. 5 is almost constant] to the exponent  $\gamma - \nu_\lambda \approx 0.672$  for  $\varepsilon \rightarrow 0$ . For a restricted range of  $\varepsilon$ , such as  $0.02 \leq \varepsilon \leq 0.1$ , this crossover may show up as an effective exponent in between these values, and indeed, such an effective exponent (namely  $\approx 1.0$ ) is observed [27]. However, in view of Fig. 5 it would be clearly wrong to take such an effective exponent as the asymptotic result, as done in [25].

It turns out that for an analysis of the critical behavior of  $\Lambda(T)$  as displayed in Fig. 5 both the non-critical background  $\Lambda_b(T)$  in Eq. (6) needs to be estimated, and the finite-size rounding of the singularity of  $\Delta\Lambda(T)$  needs to be taken into account. In view of this difficulty Das et al. [26,27] tested the consistency of the simulation results with the following finite-size scaling description

$$\Delta\Lambda(T) = QT * W(y)\varepsilon^{-\nu_\lambda}, \quad y = L / \xi, \quad (20)$$

where  $Q$  is a universal amplitude, also predicted from the theories [16-22,39], namely  $Q = (2.8 \pm 0.4) \times 10^{-3}$  [27], and  $W(y)$  is a scaling function with the limiting properties  $W(y \rightarrow \infty) = 1$  and  $W(y \rightarrow 0) \approx W_0 y^{x_\lambda}$ , with  $W_0$  an amplitude factor while  $x_\lambda = \nu_\lambda / \nu$ .

To test for the validity of Eq. (20), it is convenient to assume various trial values for  $\Lambda_b^{eff} = \Lambda_b(T_c)$  and plot the resulting estimates for the scaled part  $\varepsilon^{\nu_\lambda} \Delta\Lambda(T) = QT * W(y)$  versus  $y$ . When one achieves optimal data collapse, for small  $y$  a power law proportional to  $y^{x_\lambda}$  should emerge, while for large  $y$  a crossover towards a constant should be visible, from which an estimate for the amplitude  $Q$  could be extracted.

This strategy is tried in Fig. 6. For convenience of plotting, we choose  $y/(y_0 + y)$  with  $y_0 = 7$  rather than  $y$  as an abscissa variable (since this variable approaches unity when  $y \rightarrow \infty$ ), and display four possible assignments of  $\Lambda_b^{eff}$ . The filled symbols represent the data at  $T^* = 1.48$  for systems sizes  $L/\sigma = 7.37, 11.70, 14.74$  and  $18.57$ : their reasonably good collapse onto the remaining data (all for  $L/\sigma = 18.57$ , for different  $T^*$ ) and their approach to zero for small  $y$ , serve to justify the estimate  $\Lambda_b^{eff} = (3.3 \pm 0.8) \times 10^{-2}$ ; furthermore, the flat part for large  $y$  is indeed close to the theoretical value for  $Q$ , quoted above, and highlighted by arrows in Fig. 6. From the simulation alone, one would arrive at an estimate  $Q = (2.7 \pm 0.4) \times 10^{-3}$ , in almost perfect coincidence with the theoretical value!

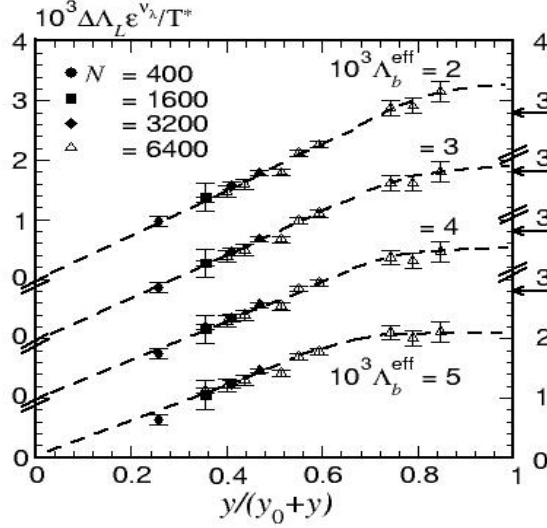


Fig. 6: Finite-size scaling plots of  $10^3 \Delta \Lambda_L(T) \varepsilon^{\nu_2}/T^*$ , the critical part of the reduced interdiffusion Onsager coefficient, versus  $y/(y_0 + y)$  where  $y = L / \xi(T)$  and  $y_0 = 7$ . The exponent estimate  $\nu_2 = 0.567$  has been adopted. The solid arrows on the right-hand axis indicate the theoretical estimate for the amplitude  $Q$ ; see text. From Das et al. [27].

More recently, Das et al. [40] analyzed a theoretical prediction [39] of the background term  $\Lambda_b^{eff}$  and found that the value obtained from the above fit is nicely compatible with this analysis [39,40]. Thus, both the constants  $Q$  and  $\Lambda_b^{eff}$  deduced from this fit appear to be physically significant.

#### 4. Conclusions and Discussions

In this paper a comprehensive simulation study of a model for a fluid binary mixture with a critical point of fluid-fluid demixing was described. It was shown that methodological advances, such as combination of SGMC and MD, and analysis techniques based on finite-size scaling, allow a rather complete analysis of both static and dynamic critical properties of the model. While the self-diffusion coefficient is nonsingular at the critical point, the behavior of the interdiffusion coefficient is more subtle: the critical vanishing is less strong than expected from the van Hove conventional theory, due to a diverging Onsager coefficient. Far away from  $T_c$ , this behavior is masked by a nonsingular background term in the Onsager coefficient. In this way, theoretical predictions, experiments, and simulation results can be reconciled with one another.

This work also shows that MD techniques are now available that can explore the critical dynamics of simple model systems. We expect that in the future it will become possible to carry out analogous studies for chemically realistic models of simple materials, as well as to extend our approach to critical behavior in complex fluids. But

one has to be aware of the fact that finite-size effects turn out to be much more pronounced in simulating dynamic critical behavior than for static critical properties [26,27,40].

Acknowledgements: Two of the authors (M. E. F. and S. K. D.) have received support from the National Science Foundation under Grant No CHE 03-01101. S. K. D. also acknowledges financial support from the Deutsche Forschungsgemeinschaft (DFG) via Grant No Bi314/18-2.

## References

- [1] W. van Gool (Ed.) Fast Ion Transport in Solids, North-Holland, Amsterdam, 1973.
- [2] G. E. Murch, Atomic Diffusion Theory in Highly Defective Solids, Trans Tech House, Adermannsdorf, 1980.
- [3] M. C. Tringides (Ed) Surface Diffusion, Atomistic and Collective Processes, Plenum Press, New York, 1997.
- [4] J. Kärger, P. Heitjans, P. Haberlandt (Eds.) Diffusion in Condensed Matter, Vieweg, Wiesbaden, 1998.
- [5] G. Kostorz (Ed) Phase Transformations in Materials, Wiley-VCH, Berlin, 2001.
- [6] K. Binder, W. Kob, Glassy Materials and Disordered Solids, World Scientific, Singapore, 2005.
- [7] A. Sadiq, K. Binder, Surface Science 128 (1983) 250 – 382.
- [8] K. W. Kehr, K. Binder, S. M. Reulein, Phys. Rev. B 39 (1989) 4891-4901.
- [9] A. De Virgiliis, K. Binder, Phys. Rev. B 73 (2006) 134205, 1-15.
- [10] P. C. Hohenberg, B. I. Halperin, Rev. Mod. Phys. 49 (1977) 435-479.
- [11] A. Onuki, Phase Transition Dynamics, Cambridge University Press, Cambridge, 2002.
- [12] M. E. Fisher, Rev. Mod. Phys. 46 (1974) 597-616.
- [13] J. Zinn-Justin, Phys. Rep. 344 (2001) 159-178.
- [14] K. Binder, E. Luijten, Phys. Rep. 344 (2001) 179-253.
- [15] K. Binder, Phys. Rev. B 15 (1977) 4425-4447.
- [16] L. P. Kadanoff, J. Swift, Phys. Rev. 166 (1968) 89–101.
- [17] K. Kawasaki, Phys. Rev. A1 (1970) 1750–1757.
- [18] L. Mistura, J. Chem. Phys. 62 (1975) 4571–4572.
- [19] J. Luettmer-Strathmann, J. V. Sengers, G. A. Olchowy, J. Chem. Phys. 103 (1995) 7482-7501.
- [20] A. Onuki, Phys. Rev. E 55 (1997) 403-420.
- [21] E. D. Siggia, B. I. Halperin, P. C. Hohenberg, Phys. Rev. B 13 (1976) 2110-2123.
- [22] R. Folk, G. Moser, Phys. Rev. Lett. 75 (1995) 2706-2709.
- [23] H. C. Burstyn, J. V. Sengers, Phys. Rev. A 25 (1982) 448-465.
- [24] R. Kutner, K. Binder, K. W. Kehr, Phys. Rev. B 26 (1982) 2967-2980.
- [25] K. Jagannathan, A. Yethiraj, Phys. Rev. Lett. 93 (2004) 015701, 1-4.
- [26] S. K. Das, M. E. Fisher, J. V. Sengers, J. Horbach, K. Binder, Phys. Rev. Lett. 97 (2006) 025702, 1-4.

- [27] S. K. Das, J. Horbach, K. Binder, M. E. Fisher, J. V. Sengers, *J. Chem. Phys.* 125 (2006) 024506, 1-12.
- [28] K. Binder, *Phys. Rev. Lett.* 45 (1980) 811-814.
- [29] J. G. Briano, E. D. Glandt, *J. Chem. Phys.* 80 (1984) 3336-3343.
- [30] A. Sariban, K. Binder, *J. Chem. Phys.* 86 (1987) 5859-5873.
- [31] M. P. Allen, D. J. Tildesley, *Computer Simulation of Liquids*, Clarendon Press, Oxford, 1987.
- [32] S. K. Das, J. Horbach, K. Binder, *J. Chem. Phys.* 119 (2003) 1547-1558.
- [33] M. E. Fisher, in M. S. Green (Ed.) *Critical Phenomena*, Academic Press, London, 1971, pp. 1-99.
- [34] K. Binder, *Z. Phys. B* 43 (1981) 119-140.
- [35] V. Privman (Ed.) *Finite Size Scaling and Numerical Simulation of Statistical Physics*, 2nd ed., Cambridge, 2005.
- [36] D. P. Landau and K. Binder, *A. Guide to Monte Carlo Simulations in Statistical Physics*, 2nd ed. (Cambridge University Press, Cambridge, 2005).
- [37] N. B. Wilding, *J. Phys.: Condens. Matter* 9 (1997) 585-612.
- [38] J.-P. Hansen, I. R. McDonald, *Theory of Simple Liquids*, Academic, London, 1986.
- [39] H. C. Burstyn, J. V. Sengers, J. K. Bhattacharjee, R. A. Ferrell, *Phys. Rev. A* 28 (1983) 1567-1578.
- [40] S. K. Das, J. V. Sengers, M. E. Fisher (to be published).